Eugene E. Pearson

NATIONAL ADVISORY COMMITTEE FOR AERONAUTICS

TECHNICAL NOTE

No. 1390

EFFECT OF COMPRESSIBILITY ON THE DISTRIBUTION OF PRESSURES OVER A TAPERED WING OF NACA 230-SERIES AIRFOIL SECTIONS

By E. O. Pearson, Jr.

Langley Memorial Aeronautical Laboratory
Langley Field, Va.

Washington
July 1947

NATIONAL ADVISORY COMMITTEE FOR AERONAUTICS

TECHNICAL NOTE NO. 1390

EFFECT OF COMPRESSIBILITY ON THE DISTRIBUTION OF PRESSURES OVER A TAPERED WING OF NACA 230-SERIES AIRFOIL SECTIONS

By E. O. Pearson, Jr.

SUMMARY

The results of pressure-distribution measurements made during high-speed wind-tunnel tests of a tapered wing of NACA 230-series airfoil sections are presented for angles of attack ranging from 0.2° to 21.2° and for free-stream Mach numbers ranging from 0.2 to about 0.7.

The peak values of minimum pressure coefficient attained were found to correspond to local Mach numbers of 1.2 to 1.4 except at angles of attack near the low-speed stall. The highest local Mach number measured was 1.55.

In most cases noticeable flow separation was indicated only at stream Mach numbers exceeding those at which peak minimum pressure coefficients were reached.

At large angles of attack corresponding to those very near the low-speed stall there was some indication that the flow about the wing broke down when the critical pressure coefficient was reached.

A comparison of measured and calculated chordwise pressure distributions for several stations along the span showed satisfactory agreement for purposes of structural design up to the critical Mach number.

INTRODUCTION

A knowledge of the magnitude of surface pressures and their distribution along the chord and span of wings at high speeds is required for proper structural design. Because of the lack of an adequate theory for determining the pressures on airfoils at supercritical speeds, the required information must be obtained entirely by experiment. The purpose of the present paper, which gives the

detailed results of extensive pressure measurements over a tapered wing of NACA 230-series airfoil sections, is to add to the existing amount of high-speed pressure-distribution data, which are very limited in extent, particularly for finite wings.

The pressure-distribution measurements reported herein were made during tests in the Langley 16-foot high-speed tunnel conducted primarily to determine the effects of Mach number on maximum lift and spanwise load distribution of a tapered wing of NACA 230-series airfoil sections. The force measurements and the spanwise load distributions obtained from the pressure measurements presented herein were reported in reference 1.

SYMBOLS

a_o free-stream speed of sound, feet per second

a local speed of sound, feet per second

A aspect ratio

α corrected angle of attack of root section (section at plane of symmetry), degrees

b wing span, feet

c airfoil chord, feet

c_{d_o} section profile-drag coefficient

c_n section normal-force coefficient $\left(\frac{1}{c}\int_0^c (P_L - P_U)\,dx\right)$

C_L wing lift coefficient $\left(\frac{L}{qs}\right)$

γ ratio of specific heat at constant pressure to specific heat at constant volume

L wing lift, pounds

m three-dimensional lift-curve slope, per radian

m_o two-dimensional lift-curve slope, per radian

M_o free-stream Mach number (V_o/a_o)

M local Mach number (V/a)

M_{cr} critical Mach number (value of M_o when M first reaches a value of unity)

p_o free-stream static pressure, pounds per square foot

p local static pressure, pounds per square foot

P pressure coefficient $\left(\frac{p - p_o}{q_o}\right)$

P_{cr} critical pressure coefficient (value of P corresponding to $M = 1.0$)

P_{min} pressure coefficient corresponding to maximum local velocity

ρ_o free-stream mass density, slugs per cubic foot

q_o free-stream dynamic pressure, pounds per square foot $\left(\frac{1}{2}\rho_o V_o^2\right)$

S wing area, square feet

V_o free-stream velocity, feet per second

V local velocity, feet per second

x chordwise distance measured from leading edge, feet

y spanwise distance measured from plane of symmetry, feet

Subscripts:

c compressible

i incompressible

U upper surface

L lower surface

APPARATUS AND METHODS

Tests were conducted in the Langley 16-foot high-speed tunnel. The wing tested had an aspect ratio of 6, a taper ratio of 2, no dihedral, 3.18° sweepback of the quarter-chord line, and 4.2° of uniform geometric washout. The wing had an NACA 23016 airfoil section at the root and an NACA 23009 airfoil section at the construction tip. A diagrammatic sketch showing the principal dimensions of the wing is given in figure 1.

Thirty-three pressure orifices were distributed over each of six wing sections, the spanwise locations of which are given in figure 1. Also shown in figure 1 are the chordwise locations of orifices over a typical section.

Pressure tubes connecting the orifices on the wing with several multiple-tube manometers in the test chamber were brought out of the rear of the wing through a boom mounted rigidly to the wing and a movable strut. This arrangement may be seen in figure 2, which is a photograph of the wing mounted in the tunnel for the pressure-distribution tests. Pressures indicated by the manometers were recorded photographically. For a more detailed description of the model and the apparatus, see reference 1.

TESTS

Most of the test runs were made with the angle of attack held constant while the tunnel speed was varied from about 150 miles per hour to the maximum speed obtainable (not choking speed), which for wing angles of attack between 0° and 4° was approximately 520 miles per hour. The corresponding range of the free-stream Mach number was from 0.20 to about 0.70. The Reynolds number varied from 3.0×10^6 to 8.1×10^6, which corresponds roughly to that of a full-scale fighter airplane flying at the test Mach numbers at altitudes of about 35,000 to 40,000 feet. At the highest angles of attack the maximum obtainable tunnel speed was about 460 miles per hour, which corresponds to a Mach number of 0.625. A few additional test runs were made with the tunnel speed held constant while the angle of attack was varied in the region near maximum lift. The angle-of-attack range covered in the pressure-distribution tests was approximately from 0° to 21°.

Some of the tests were made at angles of attack of 2.3° and 6.7° to determine the distribution of profile drag across the span. For these tests the pressure tubes and the trailing boom were removed

from the wing, and a rake of total-pressure tubes was installed on the vertical strut downstream from the wing. With this apparatus, surveys of the wing wake were made at various points along the span. The position of the rake was kept in a plane perpendicular to the tunnel air stream and consequently the distance of the rake from the wing trailing edge varied from about 1/2 chord at the root to about $1\frac{1}{2}$ chords at the tip.

CORRECTIONS

Angles of attack given in the present paper (fig. 3) have been corrected for tunnel-wall and other effects, as explained in detail in reference 1.

Supporting struts.- The effect of the supporting struts was to increase the effective velocity at the wing position. A calibration of the tunnel with the struts installed but with the wing removed showed that the increase in velocity varied from about 4 percent near the struts to about 2 percent at the center of the tunnel. A mean value of effective velocity, weighted according to the wing area, was chosen, which represented an over-all correction of about 3 percent. Corresponding values of static pressure and dynamic pressure were used in computing pressure coefficients from the measured static pressures on the wing. This correction affects all data in figure 4 and the values of c_n in figures 5 and 6.

Because of the nonuniformity of the velocity across the tunnel, the minimum pressure coefficients shown in figure 7 for the wing station nearest the struts (station 4) are in error from this source by about 5 percent at $\alpha = 0.2^\circ$ and by about 2 percent at $\alpha = 17.5^\circ$. At this station the minimum pressure coefficients as presented are negatively too large. At station 1 (near the center of the tunnel) the minimum pressure coefficients as presented are negatively too small, and here the error is about half that quoted for station 4. The errors at stations 2, 3, 5, and 6 are smaller and the error in minimum pressure coefficient at these stations is of the order of 1 percent for all angles of attack.

Tunnel-wall interference.- Neither the pressure coefficients nor the stream Mach numbers have been corrected for tunnel-wall interference because of some uncertainties in the application of corrections to the pressure data for the present case of a relatively large finite wing in a circular tunnel; also, a check of the order

of magnitude of the errors involved by the methods of references 2 and 3 indicates that these errors do not significantly affect the conclusions reached.

The principal errors arise from the increase in effective velocity at the wing position due to constriction of the tunnel by the large wing wake at high angles of attack and high Mach numbers where the flow is largely separated. As long as the flow over the wing was smooth, the errors in pressure coefficient and Mach number from this source were found to be negligible. Under the conditions of strong shock and extensive flow separation occurring at the highest test angles of attack and Mach numbers it was determined that the indicated dynamic pressure and Mach number were too low by as much as 4 percent and 2 percent, respectively. The test point on the curve of minimum pressure coefficient against Mach number in figure 4(j), giving a pressure coefficient of -2.00 at $M_o = 0.622$, is representative of data obtained under these extreme conditions. For this point it is probable that the minimum pressure coefficient is negatively too large by about 6 percent.

Since negative pressure coefficients are too large negatively and stream Mach numbers are too low, local Mach numbers are affected by constriction to a much smaller extent than the pressure coefficients as illustrated by the following numerical example:

The equation relating local Mach number, stream Mach number, and pressure coefficient for isentropic flow is

$$M = \sqrt{\frac{2}{\gamma - 1}\left[\left(\frac{1}{1 + \frac{\gamma}{2}PM_o^2}\right)^{\frac{\gamma-1}{\gamma}}\left(1 + \frac{\gamma - 1}{2}M_o^2\right) - 1\right]}$$

Substitution of the values of pressure coefficient and Mach number previously given ($P = -2.00$, $M_o = 0.622$) in this equation gives a value of local Mach number of 1.32. If the stream Mach number is increased by 2 percent (corrected $M_o = 0.635$) and the pressure coefficient is reduced numerically by 6 percent (corrected $P = -1.88$) and these corrected values are substituted in the equation, a value of local Mach number of 1.31 is obtained. The difference between corrected and uncorrected local Mach number is seen to be less than 1 percent.

RESULTS AND DISCUSSION

Wing lift characteristics (from force tests).- The lift curves for the wing at various Mach numbers as determined from the force tests reported in reference 1 are given in figure 3 for purposes of correlation.

Pressure coefficients and section normal-force coefficients.- Chordwise pressure-distribution diagrams for stations 2 and 3 (see fig. 1 for locations) are presented in figure 4 for a range of angle of attack and Mach number. The variations with Mach number of minimum pressure coefficient and section normal-force coefficient as obtained from integration of the pressure-distribution diagrams are also shown in figure 4. In order to prevent possible confusion over two distinctly different minimum values of pressure coefficient the following definition of terms is offered: "Minimum pressure coefficient" refers to the largest negative value of pressure coefficient measured at a particular spanwise station on the wing for any angle of attack and Mach number. This minimum quantity may be obtained from the pressure-distribution diagrams of figure 4. The term "peak minimum pressure coefficient" refers to the largest negative value attained by the curves of minimum pressure coefficient plotted against Mach number, which are also given in figure 4.

Stations 2 and 3 were chosen for discussion because minimum pressure coefficients and maximum normal-force coefficients occurred in this region on the wing. The position of these minimum and maximum coefficients shifted from station 2 to station 3 as the angle of attack was increased from about 2° to that value corresponding to the stall; at $\alpha = 8.9°$ the coefficients were about the same in magnitude at both of these stations. Compare figures 4(d) and 4(e).

The curves of minimum pressure coefficient against stream Mach number for most of the angle-of-attack range (figs. 4(a) to 4(g)) show that local Mach numbers increased and local pressures decreased with increasing free-stream Mach number in the usual manner until peak minimum pressure coefficients which corresponded to local Mach numbers from 1.2 to 1.4 were reached. In general, maximum local Mach numbers and peak values of minimum pressure coefficient did not occur at the same free-stream Mach number; maximum local Mach numbers were reached at somewhat higher stream Mach numbers than peak values of minimum pressure coefficient. The maximum value of local Mach number measured was about 1.55 (fig. 4(f)).

The evidence shown in figure 4 indicates that over most of the angle-of-attack range noticeable flow separation, as indicated by a deficiency in pressure recovery near the trailing edge, did not occur

until the stream Mach number corresponding to the attainment of peak minimum pressure coefficients had been well exceeded. The normal-force coefficient, however, generally showed some departure from the smooth subcritical trend at Mach numbers only slightly in excess of the critical, even though little if any flow separation was indicated. For an example of beginning separation see the pressure distribution for a Mach number of 0.651 in figure 4(f). However, the possibility of the occurrence of a local separation confined to the region of compression shock at lower supercritical Mach numbers cannot be excluded (reference 4).

At angles of attack very near the low-speed stall (fig. 4(j)) the rather meager data appear to show that when the critical pressure coefficient is reached the flow can tolerate little if any shock disturbance without breaking down. The results on this wing presented in reference 5 more strongly corroborate this indication.

The subcritical rise in normal-force coefficient with Mach number has been compared with that given by the small-disturbance theory as applied to the finite wing by A. D. Young in a British paper of limited distribution. The equation for the ratio of normal-force coefficient at any subcritical Mach number to normal-force coefficient at $M = 0$ is as follows:

$$\frac{c_{n_c}}{c_{n_i}} \approx \frac{m_c}{m_i} = \frac{m_{o_c}}{m_{o_i}} \left(\frac{m_{o_i} + \pi A}{m_{o_c} + \pi A} \right)$$

$$\frac{c_{n_c}}{c_{n_i}} \approx \frac{1}{\sqrt{1 - M^2}} \left[\frac{m_{o_i} + \pi A}{\left(\frac{m_{o_i}}{\sqrt{1 - M^2}} \right) + \pi A} \right]$$

The value of the low-speed two-dimensional lift-curve slope m_{o_i} was taken as that for thin airfoils (2π). Upon substitution of this value for m_{o_i} the equation became

$$\frac{c_{n_c}}{c_{n_i}} \approx \frac{A + 2}{A\sqrt{1 - M^2} + 2}$$

As may be seen in figure 4 the curves calculated from the foregoing equation are in excellent agreement with the experimental normal-force-coefficient curves up to the force-break Mach number, beyond which large differences between the experimental and theoretical results are shown.

Contours of pressure coefficient over the upper surface of the wing are shown in figures 5 and 6 for several Mach numbers and for angles of attack of 2.3° and 6.7°. Included in these figures are curves showing the spanwise distribution of normal-force coefficient and profile-drag coefficient for correlation with the data given in figures 4(a) and 4(c).

These figures serve to show how the region of supersonic flow ahead of the compression shock or shocks formed and expanded with increasing Mach number. Of interest is the fact that at the highest Mach numbers (figs. 5(f) and 6(d)) the drag coefficient increased to about two or three times its low-speed value, while the normal-force coefficient remained essentially unaffected.

Comparison of theoretical and experimental chordwise pressure distributions.- The measured and calculated chordwise pressure distributions over the wing sections at six spanwise stations are given in figure 7 for a range of angle of attack and Mach number.

The chordwise pressure distributions were calculated by the method of reference 6 for each section so that the lift coefficients were in agreement with those obtained experimentally at a Mach number of about 0.2. The calculated pressure coefficients were then extrapolated to higher Mach numbers by the von Kármán-Tsien relation, which is recommended in reference 6.

The von Kármán-Tsien theory, of course, is not valid at Mach numbers higher than the critical, but the comparison is continued to supercritical speeds to show the departure of the measured flow from that predicted by the first approximation of the theory. It should be noted that such calculations lead to the impossible condition of pressure coefficients which correspond to pressures less than absolute zero.

At an angle of attack of 21.2° (fig. 7(f)) the wing was completely stalled at all Mach numbers, and consequently the calculated pressure distributions are not given for this condition.

An examination of figure 7 shows that for purposes of structural design the method of reference 6 gives results in satisfactory agreement with experiment at Mach numbers up to the critical.

Pressure distributions at sections very near the wing tip are undoubtedly distorted by the flow around the tip. For the test wing, however, the area so affected is small, as evidenced by the very small distortion at station 6 $\left(\frac{y}{b/2} = 0.94\right)$.

CONCLUSIONS

1. Peak values of minimum pressure coefficients were found to correspond to local Mach numbers of 1.2 to 1.4. Local Mach numbers generally continued to increase with increasing stream Mach number beyond that at which peak minimum pressure coefficients occurred. The maximum local Mach number measured was about 1.55.

2. In general no noticeable indication of flow separation was observed until the stream Mach number corresponding to the attainment of peak pressure coefficients had been well exceeded.

3. At angles of attack very near those corresponding to the low-speed stall there was some indication that the flow about the wing broke down when the critical pressure coefficient (local Mach number = 1.0) was reached.

4. The measured rate of increase with Mach number of section normal-force coefficient at subcritical values of Mach number was in excellent agreement with that predicted from the small-disturbance theory. Large differences between the theoretical and experimental results occurred at high supercritical speeds.

5. The method used for calculating the chordwise pressure distribution gave results in satisfactory agreement with experiment for the purpose of structural design at Mach numbers up to the critical.

Langley Memorial Aeronautical Laboratory
National Advisory Committee for Aeronautics
Langley Field, Va., May 7, 1947

REFERENCES

1. Pearson, E. O., Jr., Evans, A. J., and West, F. E., Jr.: Effects of Compressibility on the Maximum Lift Characteristics and Spanwise Load Distribution of a 12-Foot-Span Fighter-Type Wing of NACA 230-Series Airfoil Sections. NACA ACR No. L5G10, 1945.

2. Thom, A.: Blockage Corrections in a Closed High-Speed Tunnel. R. & M. No. 2033, British A.R.C., 1943.

3. Allen, H. Julian, and Vincenti, Walter G.: The Wall Interference in a Two-Dimensional-Flow Wind Tunnel with Consideration of the Effect of Compressibility. NACA Rep. No. 782, 1944.

4. Wood, Clotaire, and Zalovcik, John A.: Flight Investigation at High Speeds of Flow conditions over an Airplane Wing as Indicated by Surface Tufts. NACA CB No. L5E22, 1945.

5. Furlong, G. Chester, and Fitzpatrick, James E.: Effects of Mach Number and Reynolds Number on the Maximum Lift Coefficient of a Wing of NACA 230-Series Airfoil Sections. NACA TN No. 1299, 1947.

6. Anon: Chordwise Air-Load Distribution. ANC-1 (2), Army-Navy-Civil Committee on Aircraft Design Criteria, Oct. 28, 1942.

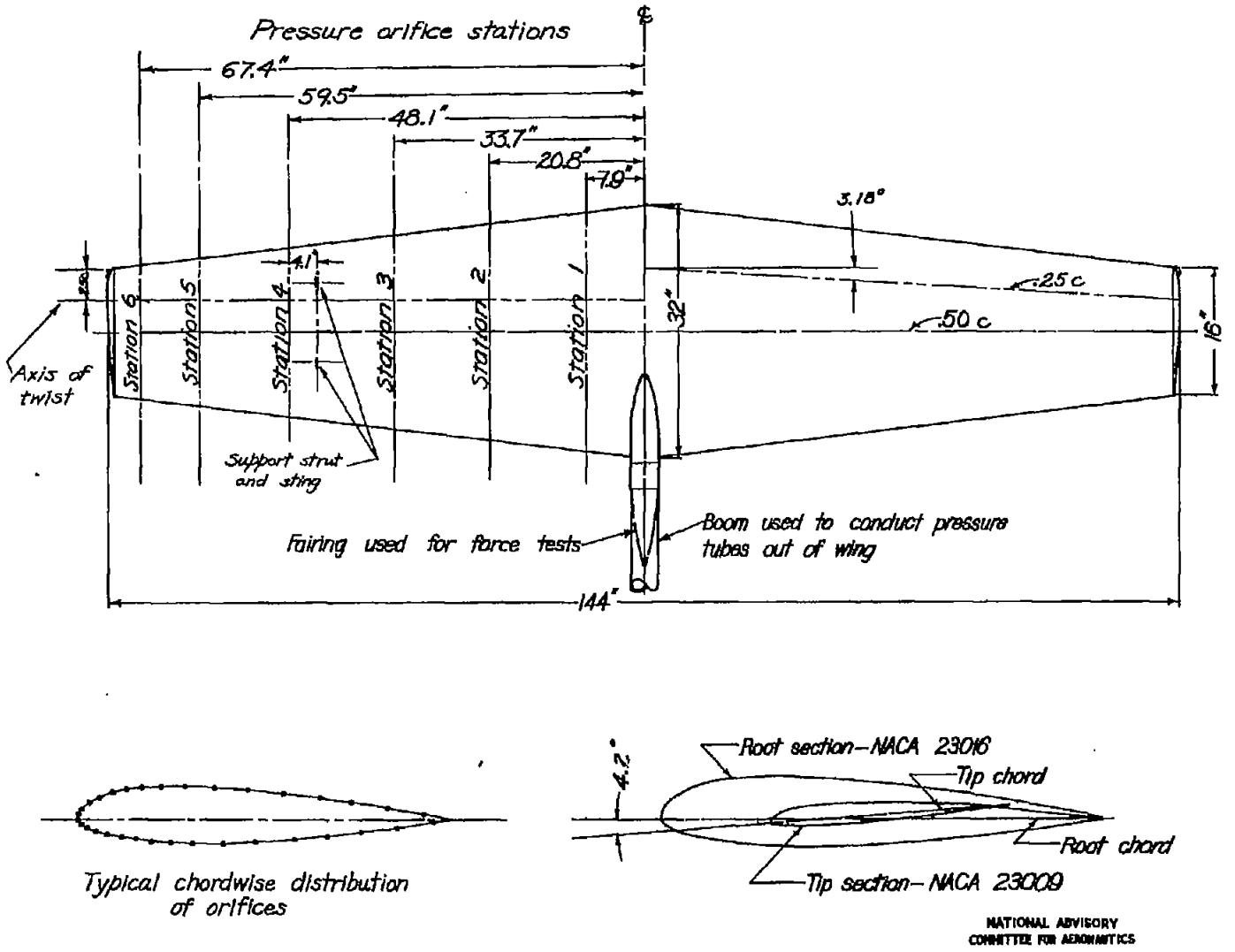

Figure 1.—Principal wing dimensions and locations of pressure orifices.

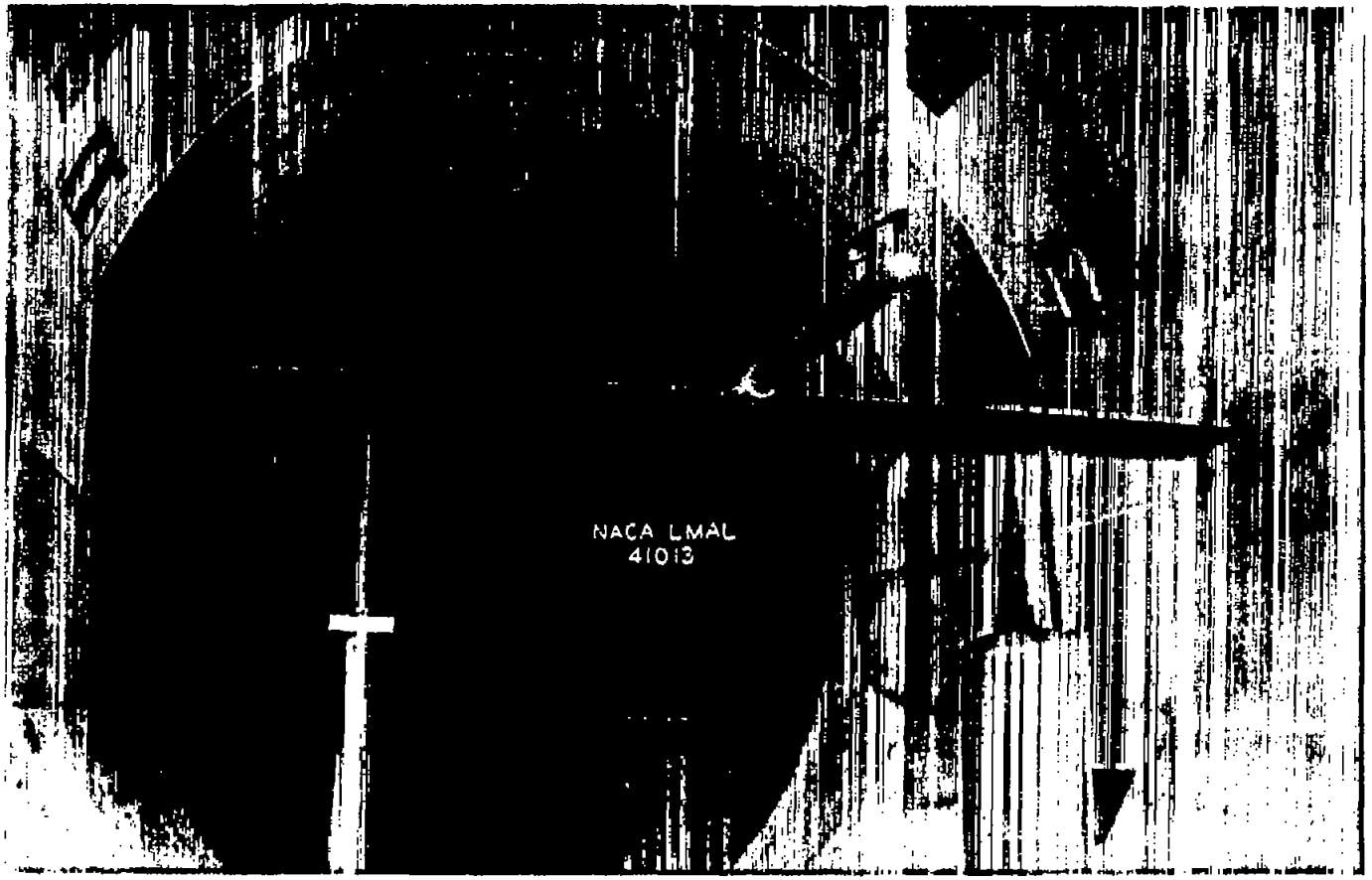

Figure 2.- Rear view of wing mounted in the tunnel for the pressure-distribution tests.

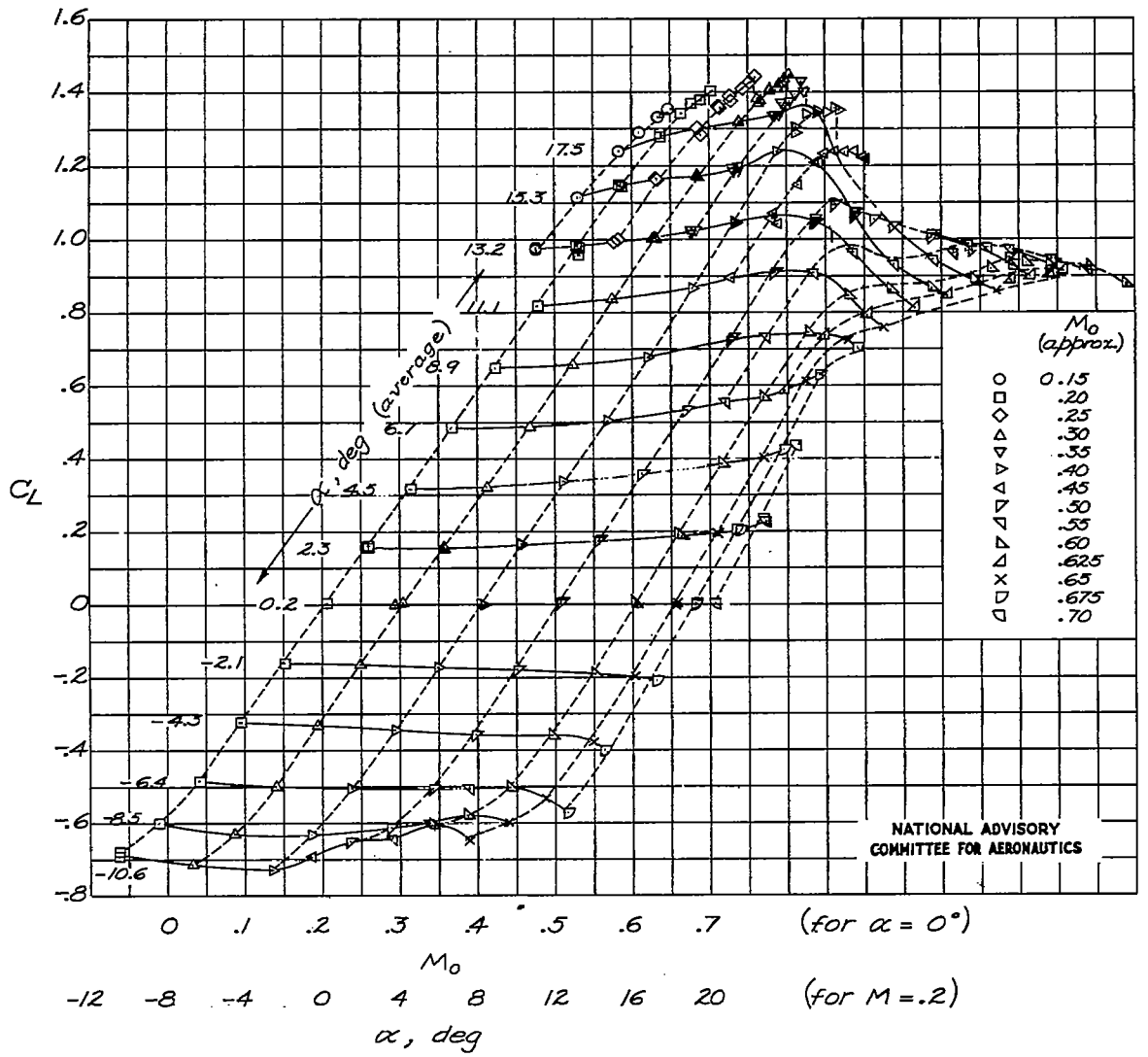

Figure 3.- Wing lift coefficient as a function of angle of attack and Mach number. (From reference 1.)

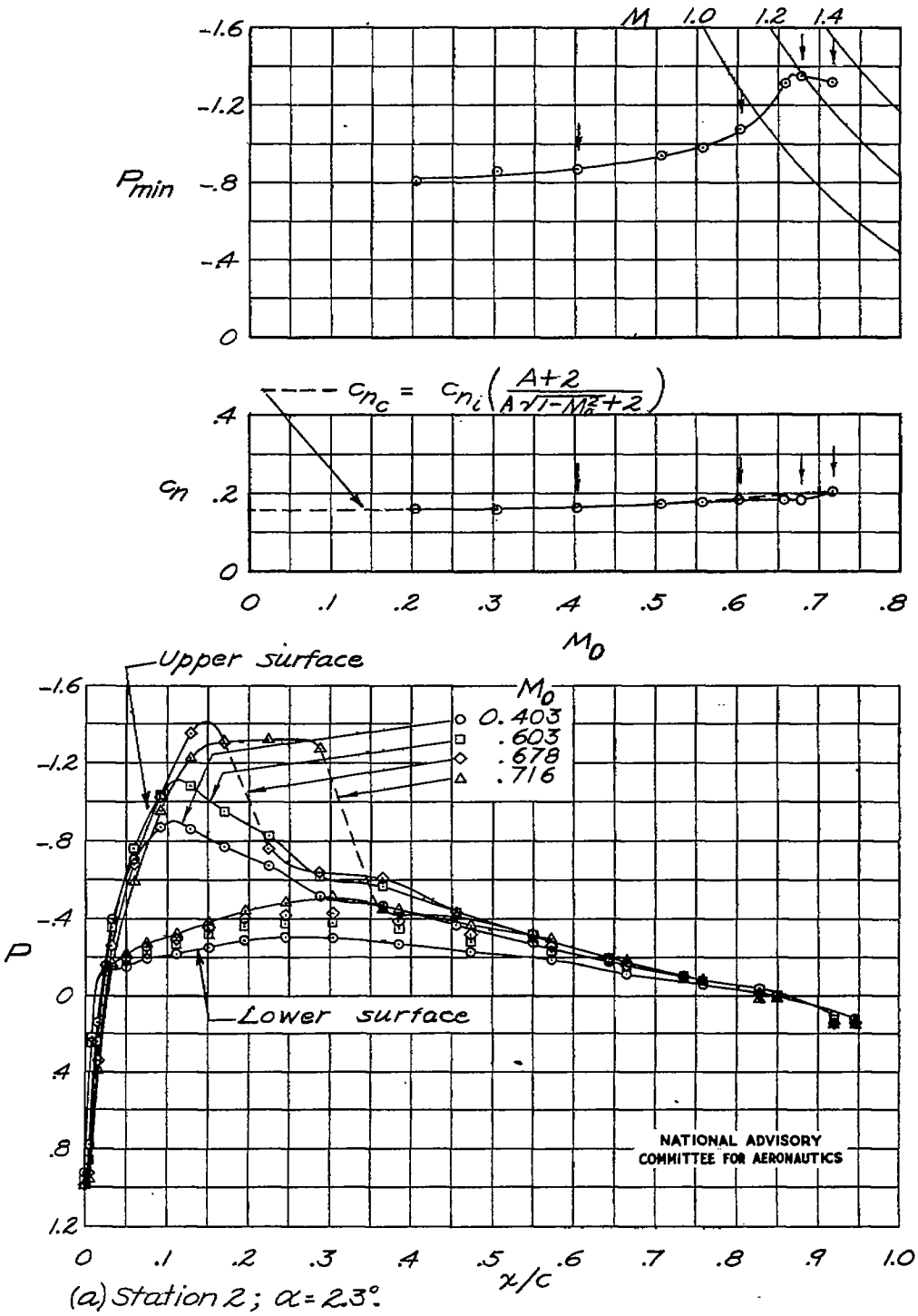

(a) Station 2; $\alpha = 2.3°$.

Figure 4.- Pressure distributions over stations 2 and 3 of fighter-type wing, with curves of minimum pressure coefficient and normal-force coefficient against Mach number.

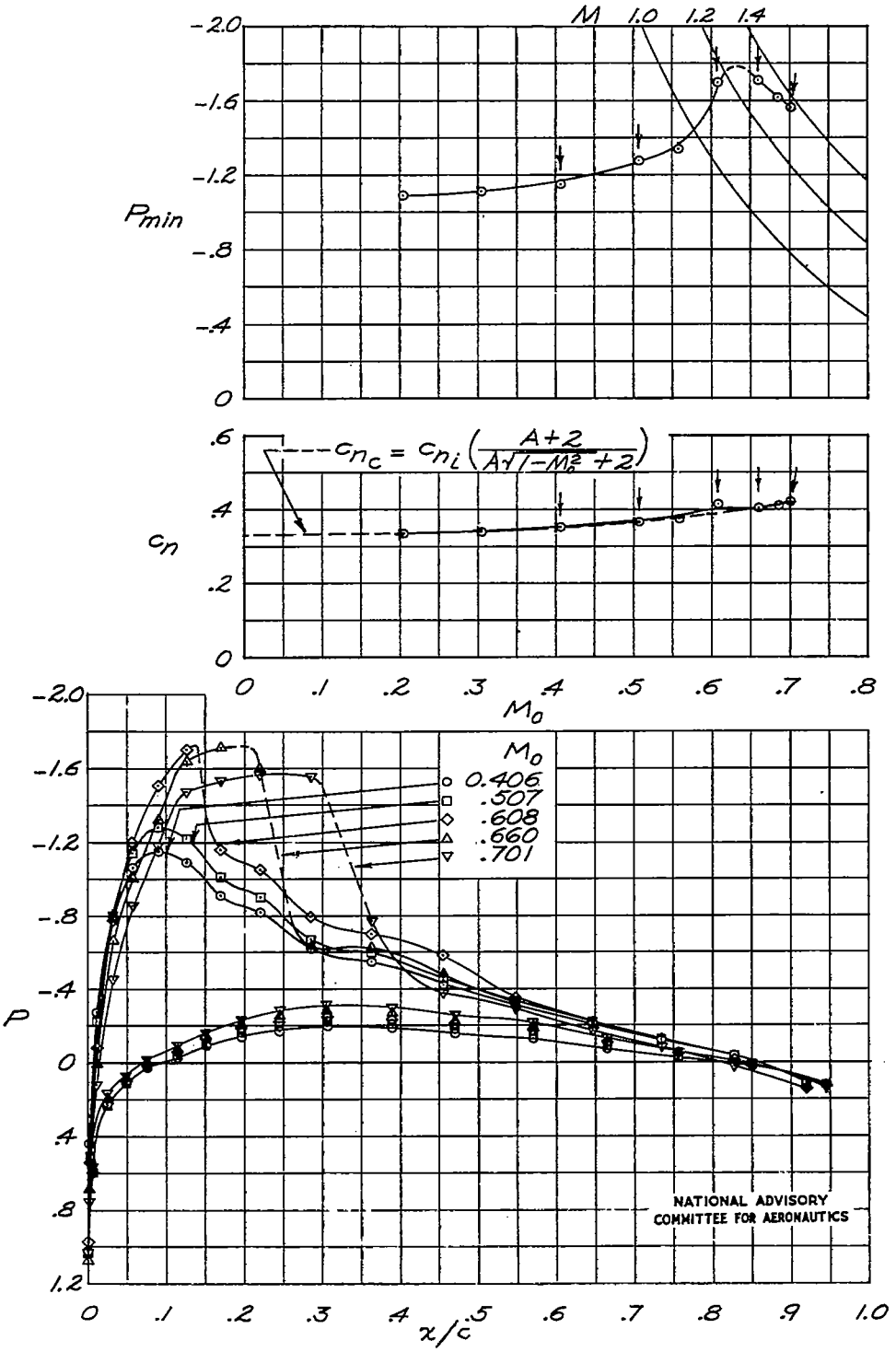

(b) Station 2; $\alpha = 45°$

Figure 4 - Continued.

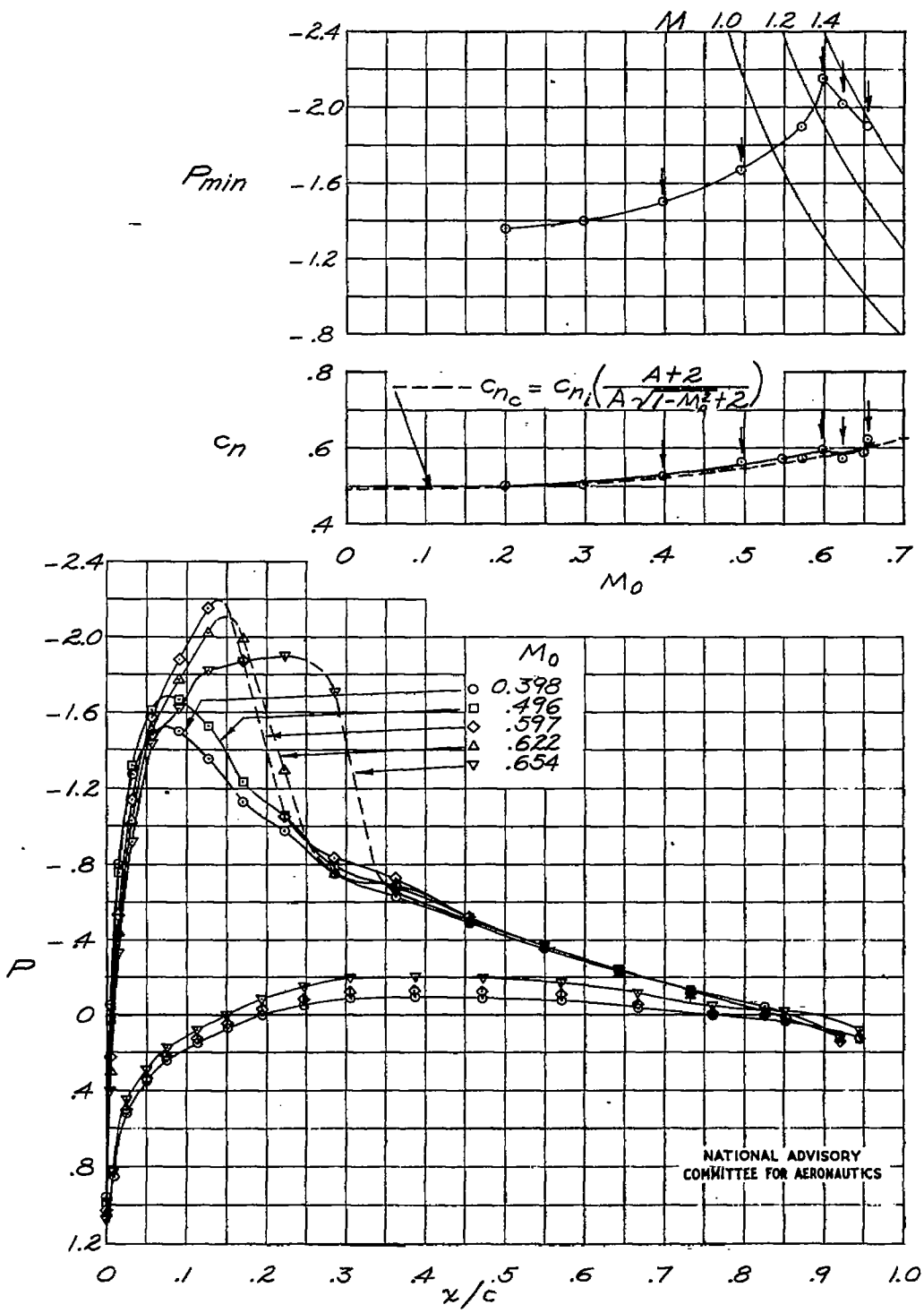

(c) Station 2; $\alpha = 6.7°$

Figure 4.- Continued.

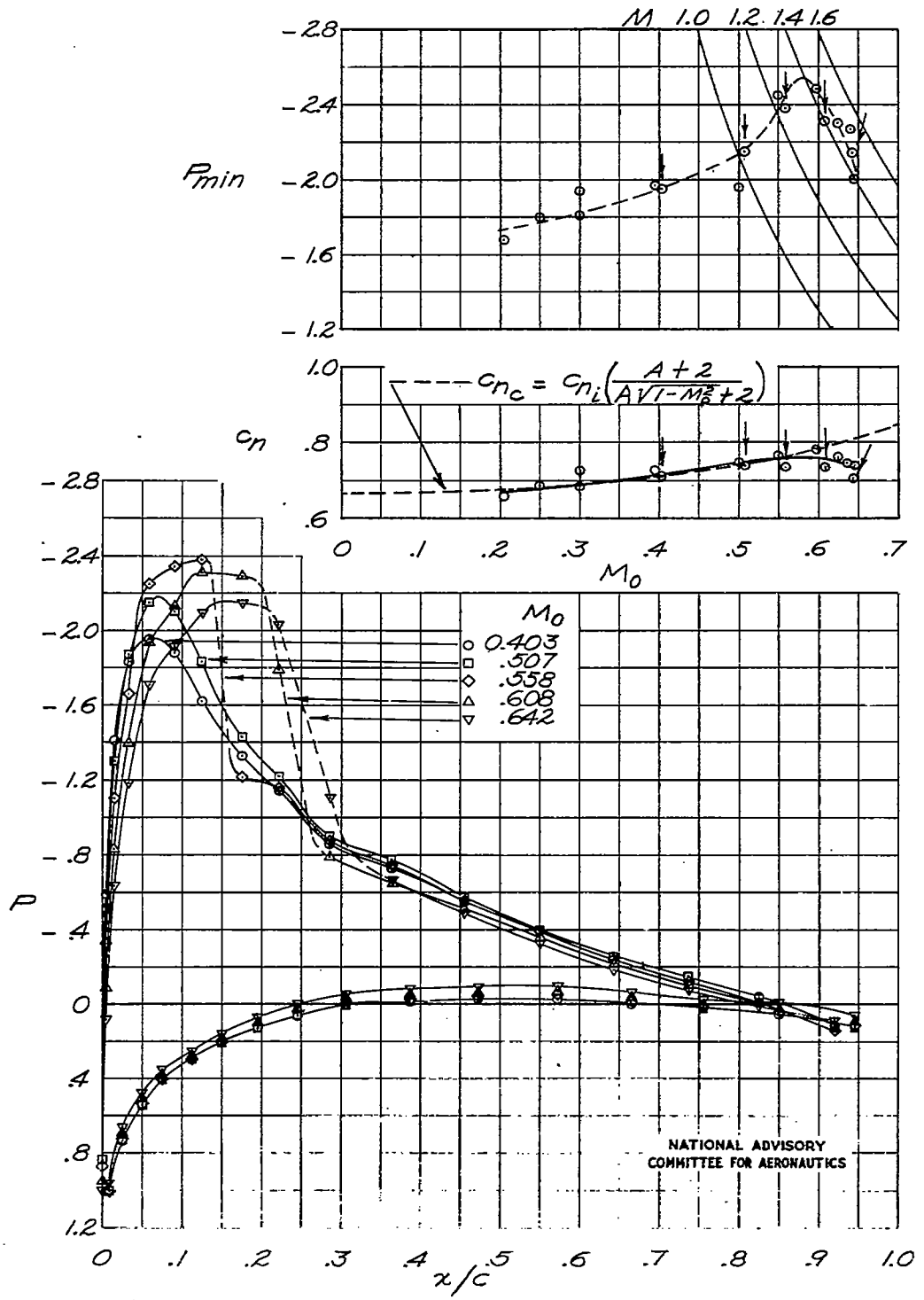

(d) Station 2; $\alpha = 8.9°$.

Figure 4.- Continued.

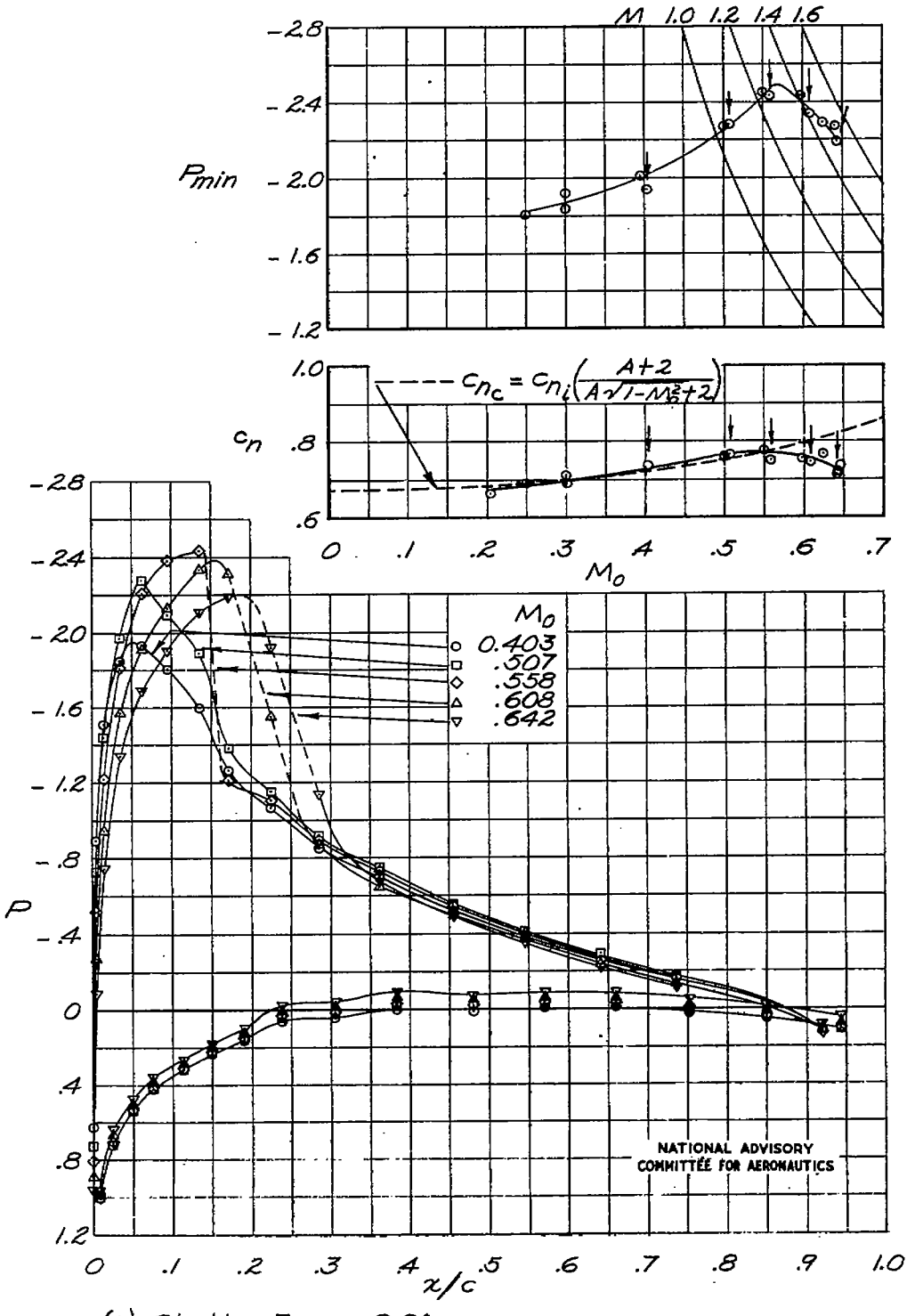

(e) Station 3; $\alpha = 8.9°$.

Figure 4.- Continued.

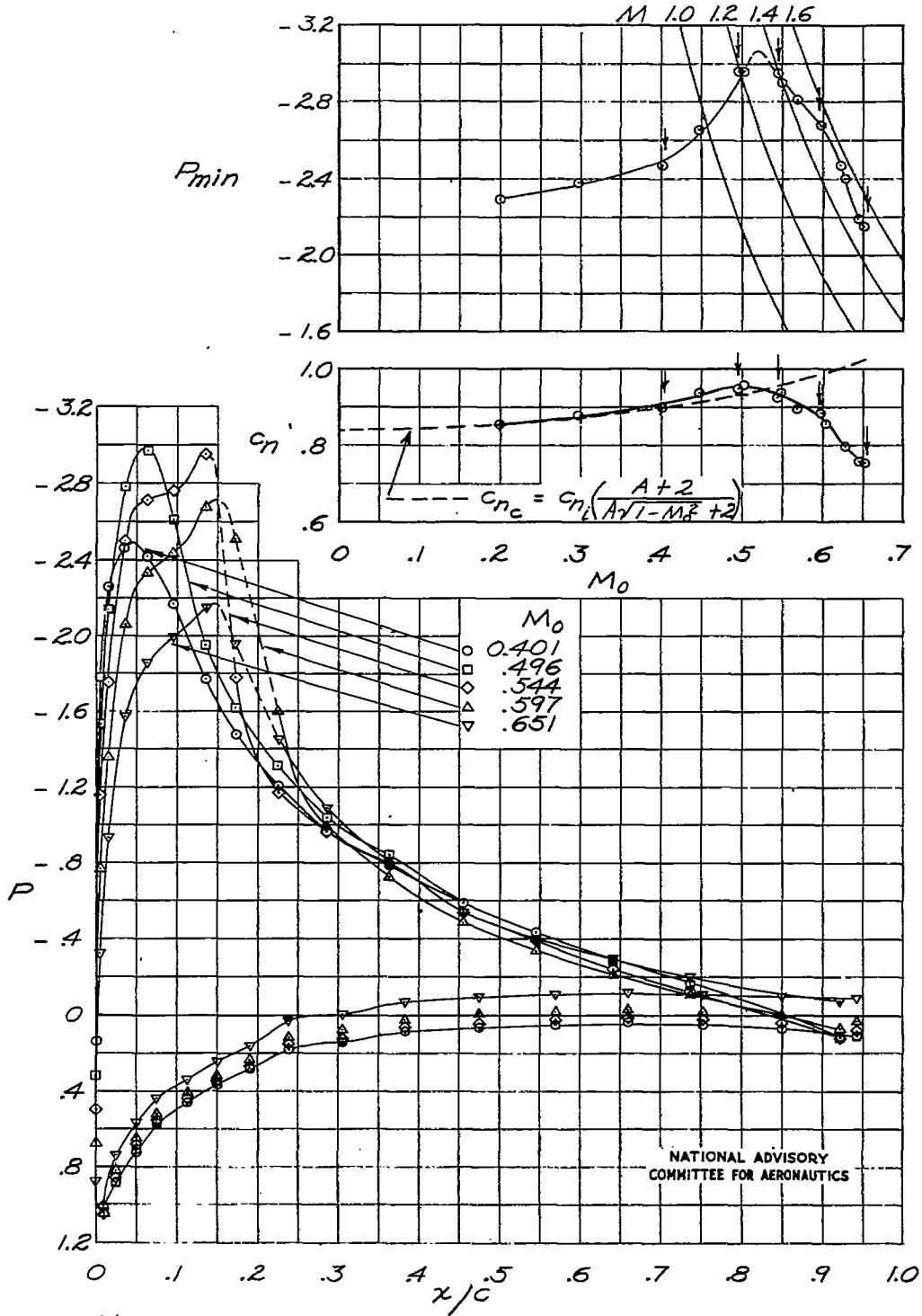

(f) Station 3 ; $\alpha = 11.1°$.

Figure 4.- Continued.

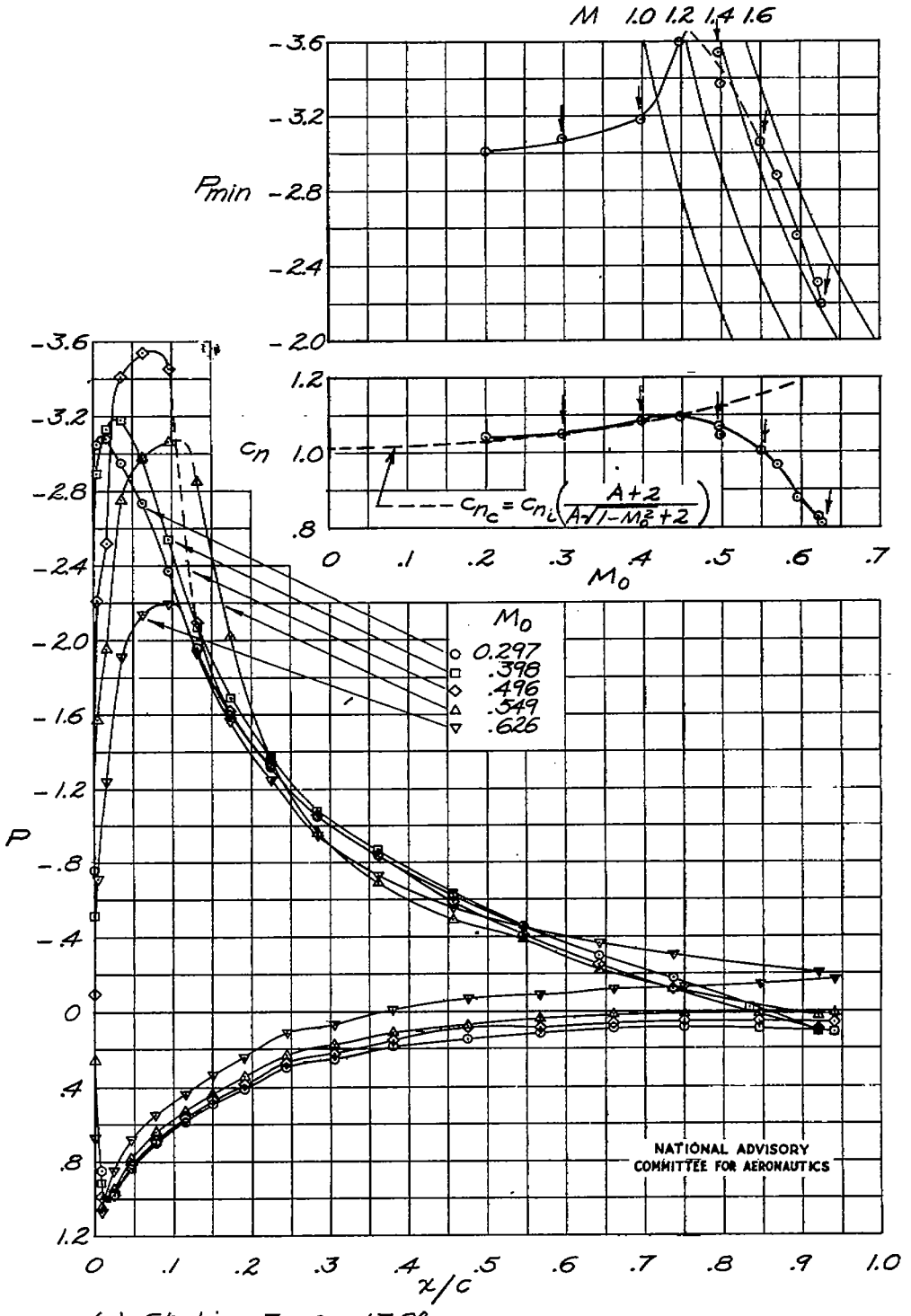

(g) Station 3 ; $\alpha = 13.2°$.

Figure 4.- Continued.

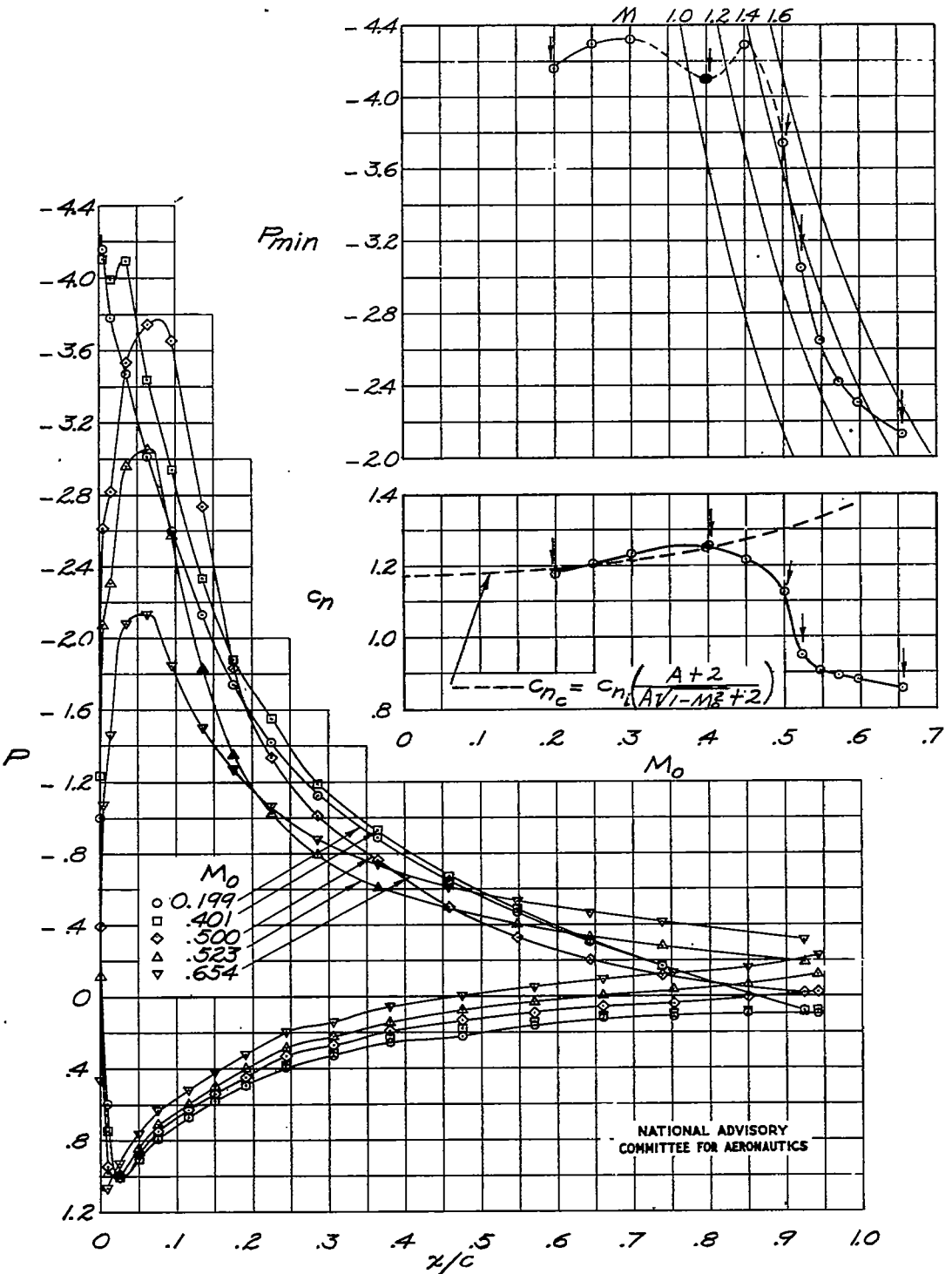

(h) Station 3; $\alpha = 15.3°$.

Figure 4.- Continued.

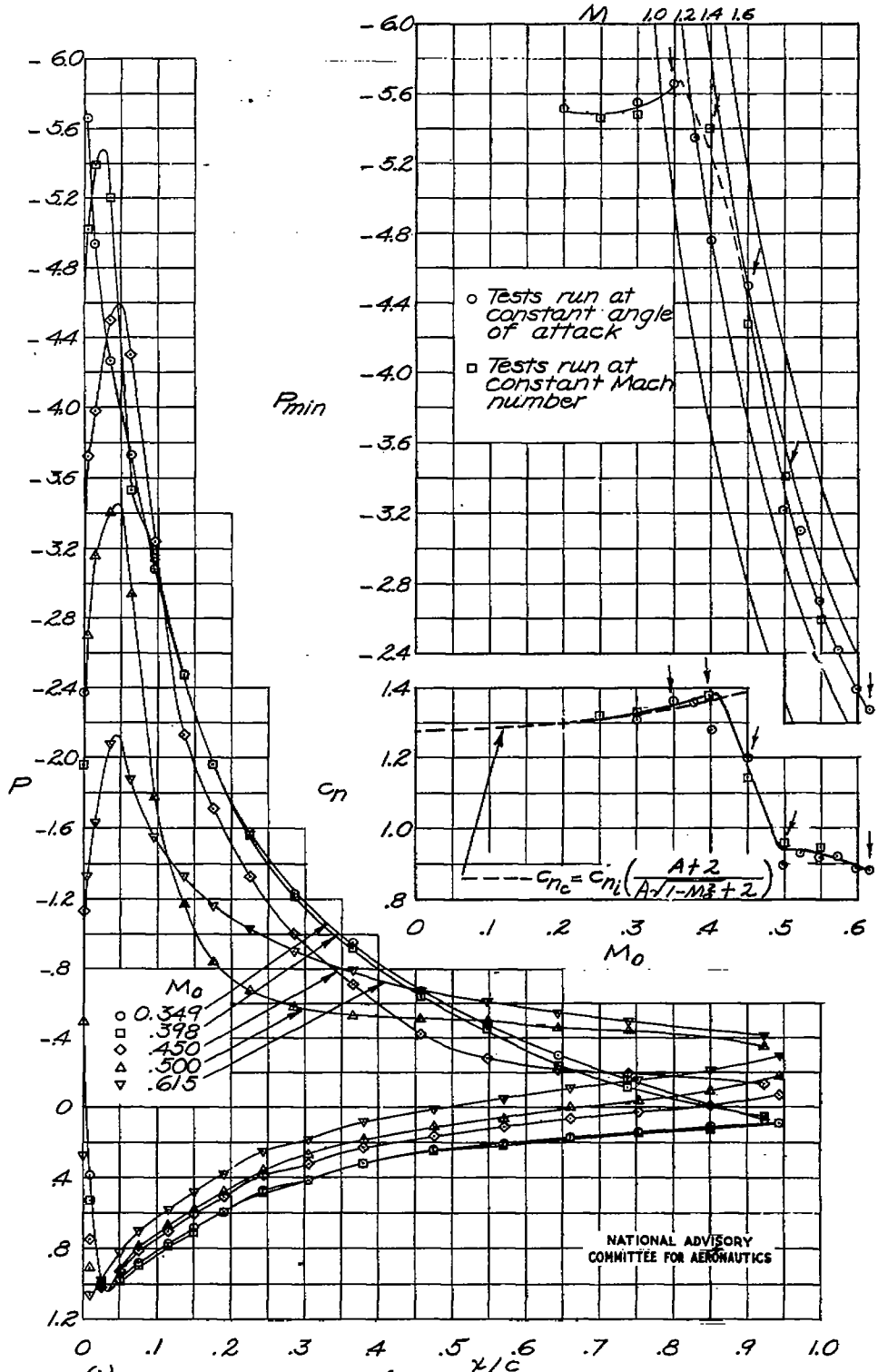

(i) Station 3; $\alpha = 17.5°$.

Figure 4.- Continued.

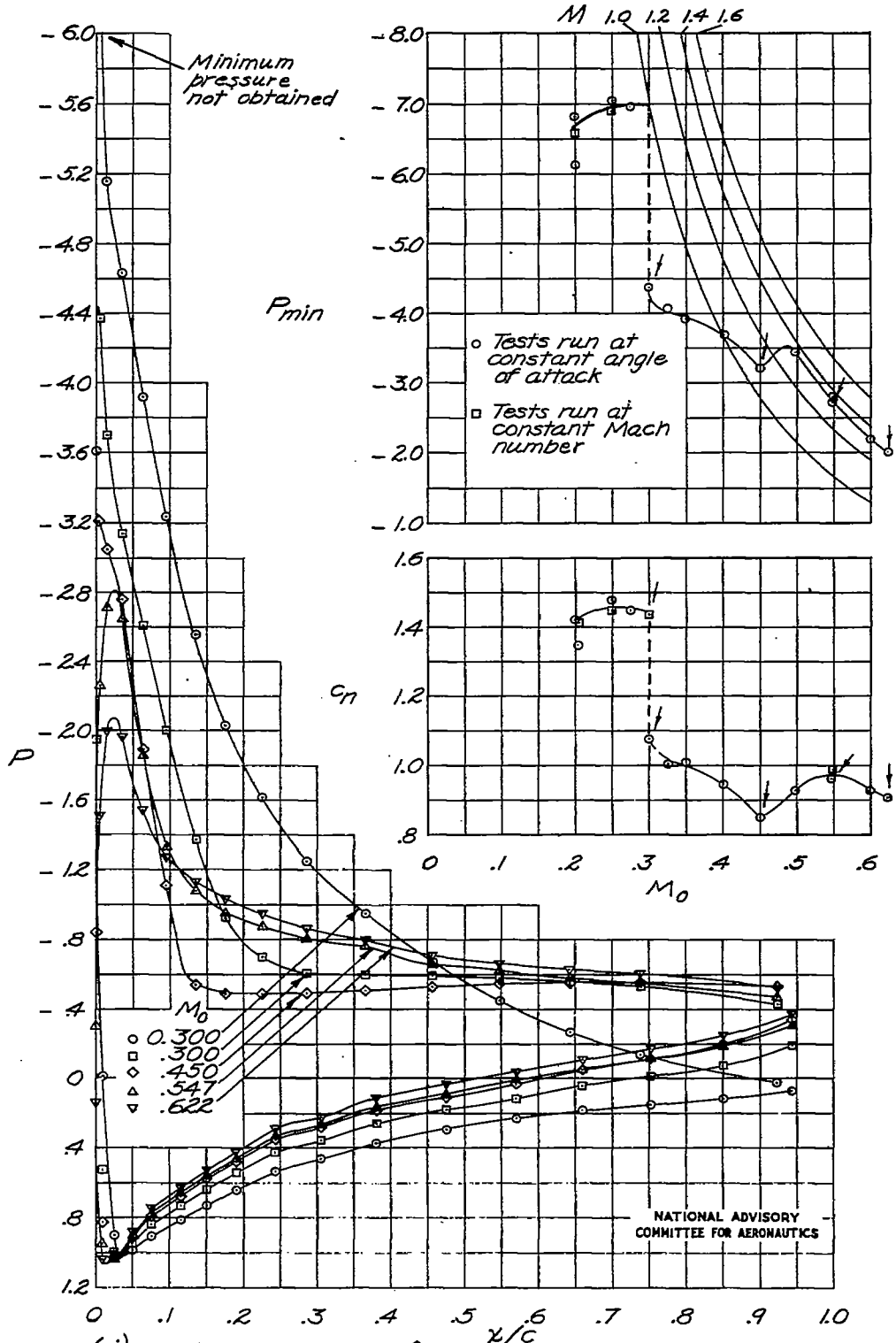

(j) Station 3; $\alpha = 19.5°$.

Figure 4.- Continued.

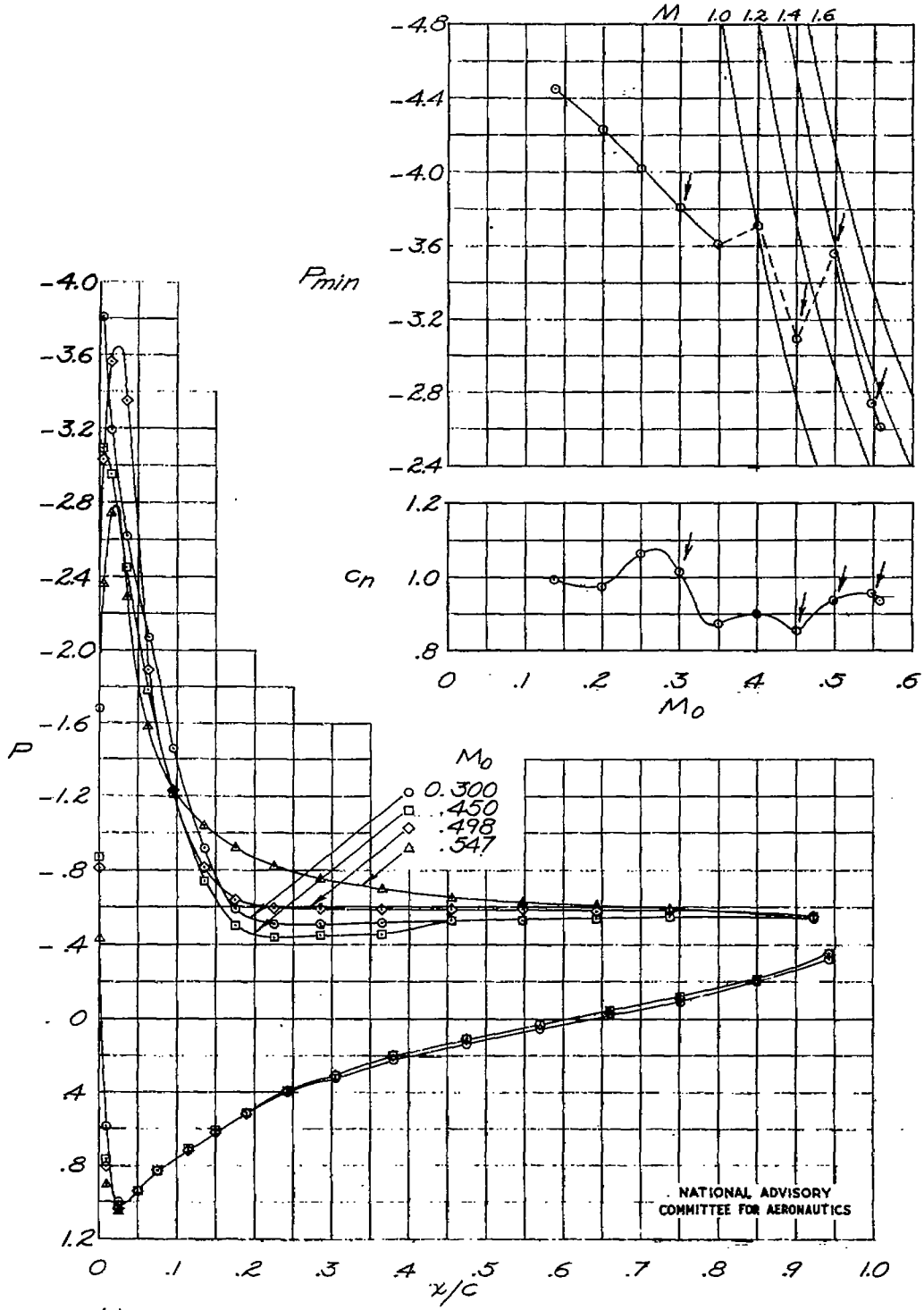

(k) Station 3 ; $\alpha = 21.2°$

Figure 4.- Concluded.

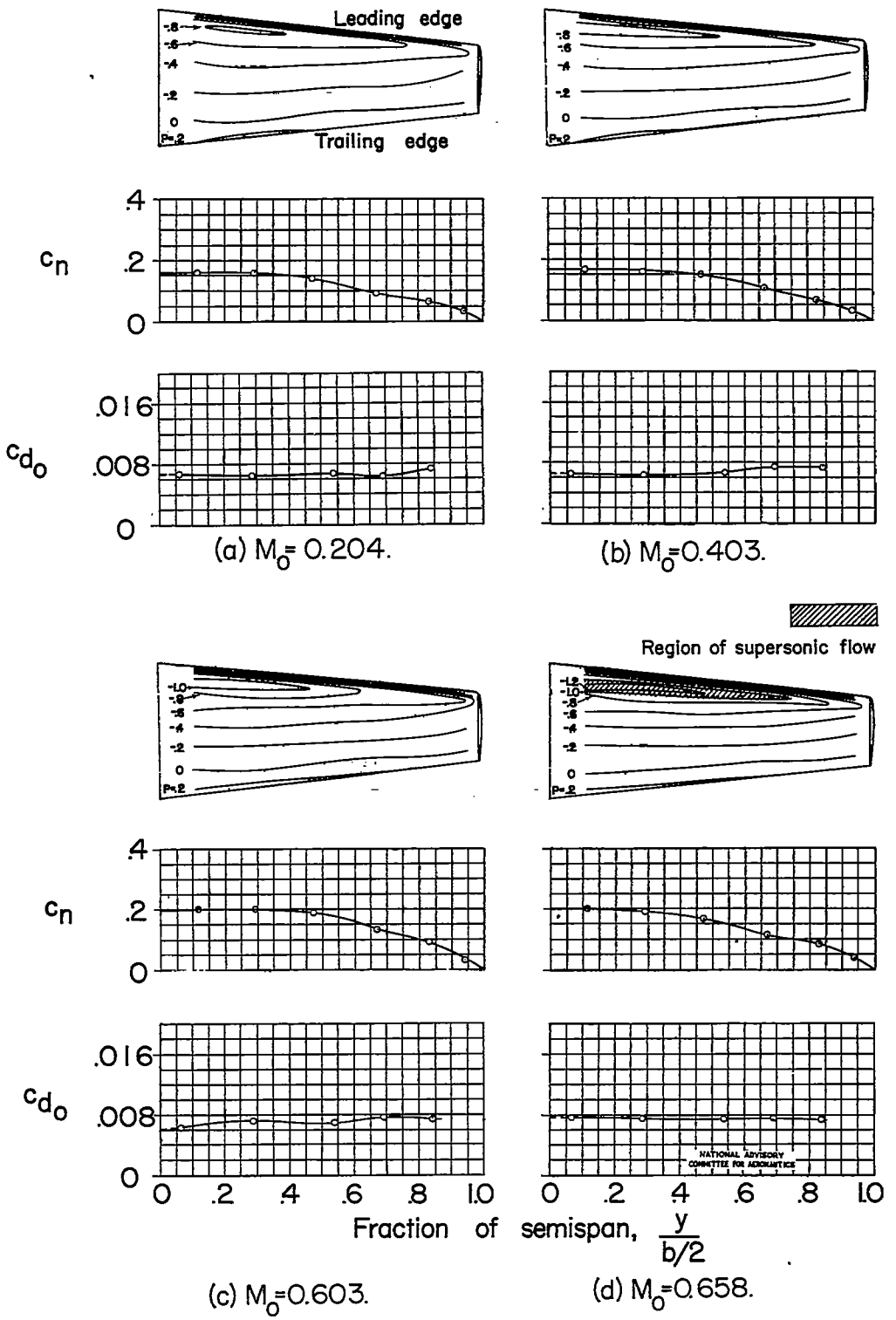

Figure 5.—Contours of pressure coefficient over upper surface of fighter-type wing and spanwise distribution of normal-force and profile-drag coefficients as affected by compressibility. $\alpha = 2.3°$.

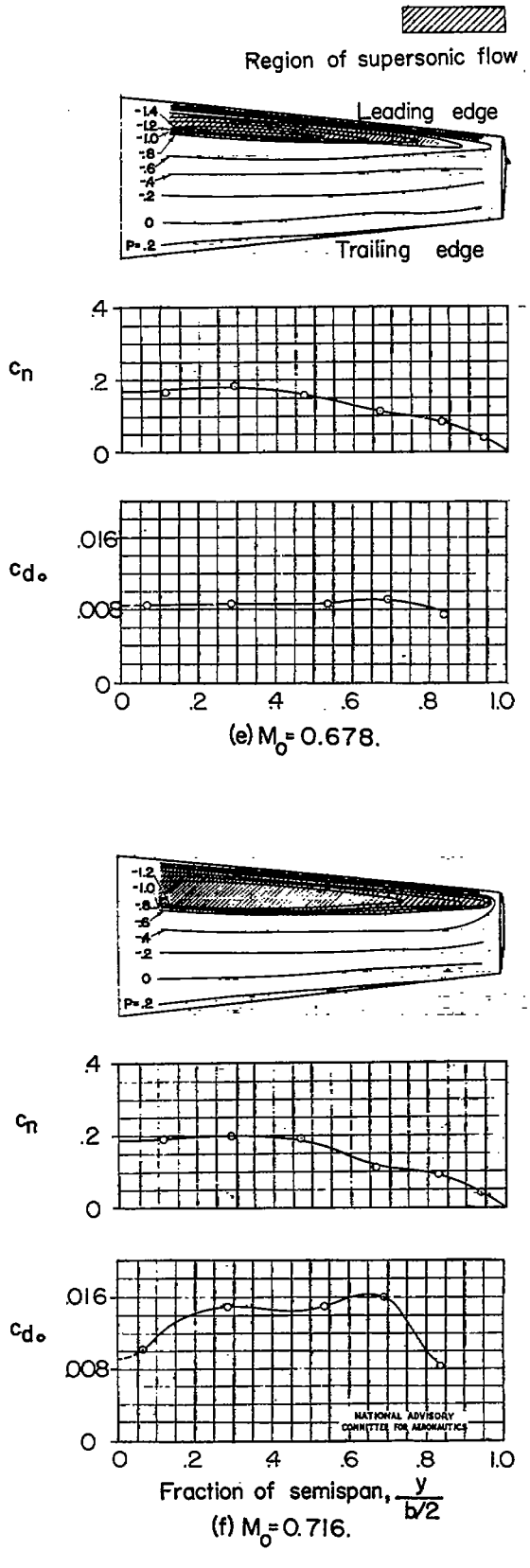

Figure 5— Concluded.

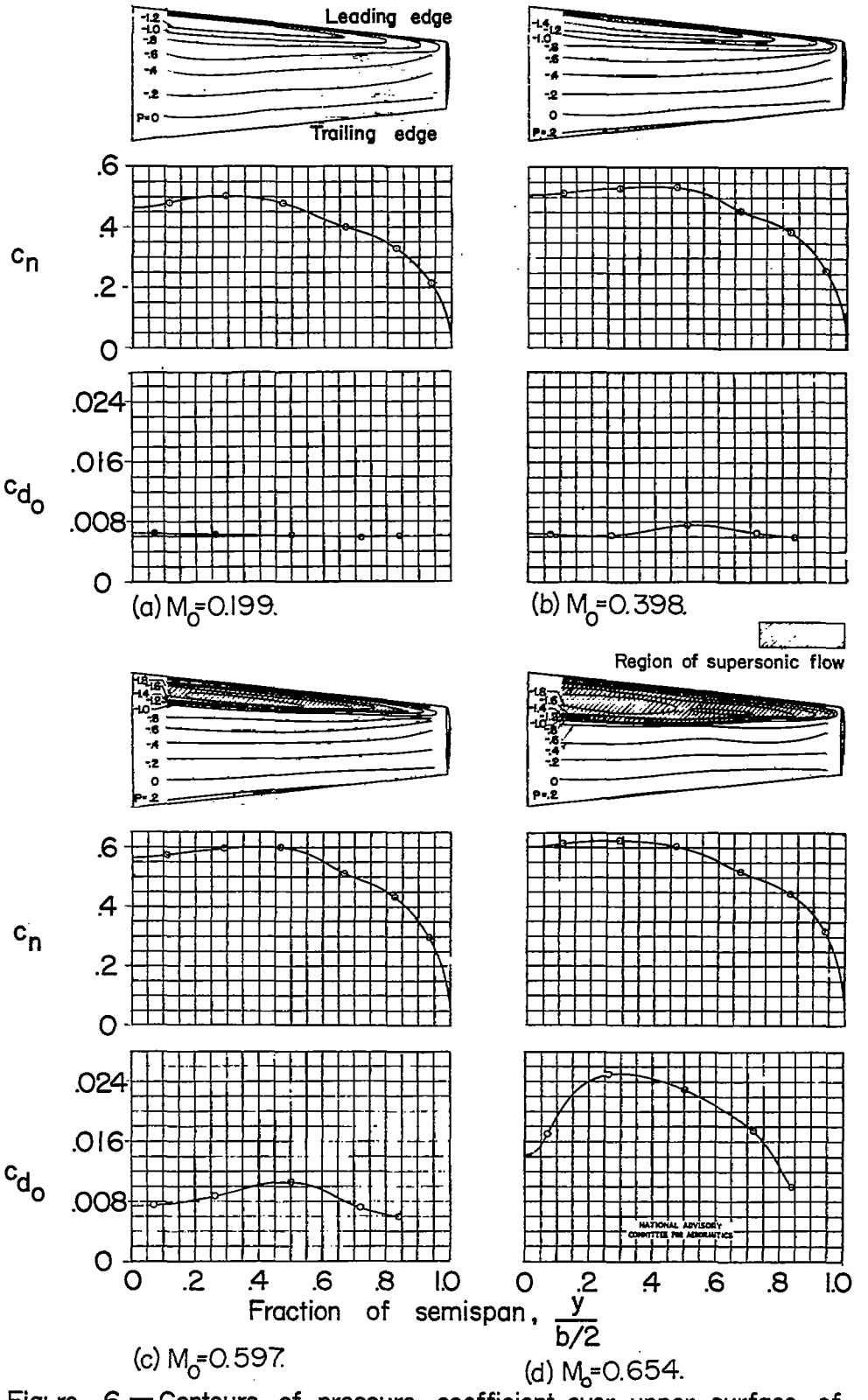

Figure 6.—Contours of pressure coefficient over upper surface of fighter-type wing and spanwise distribution of normal-force and profile-drag coefficients as affected by compressibility. $\alpha = 6.7°$

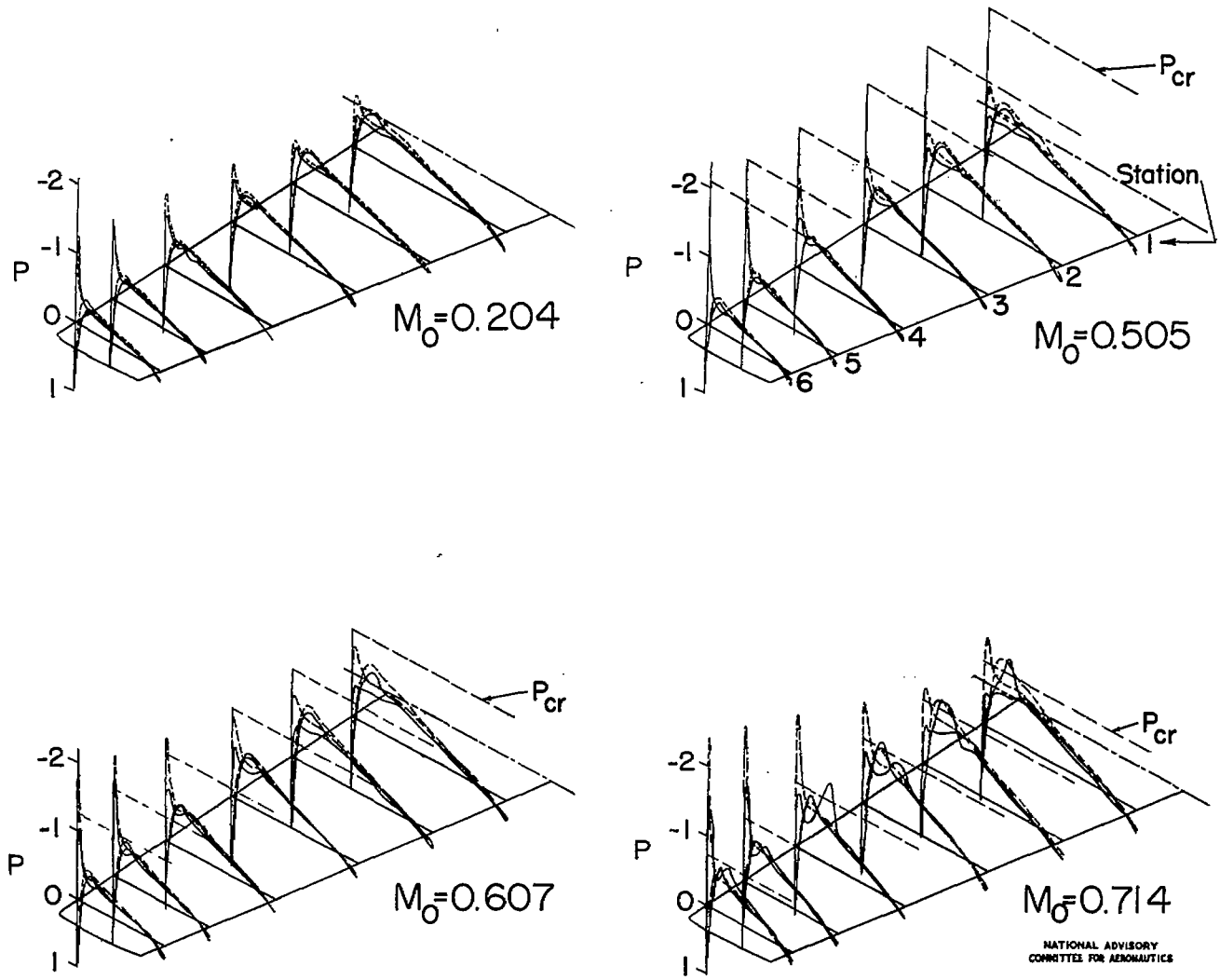

—— Measured
---- Calculated

(a) $\alpha = 0.2°$.

Figure 7.- Measured and calculated pressure distributions about fighter-type wing at various Mach numbers and angles of attack.

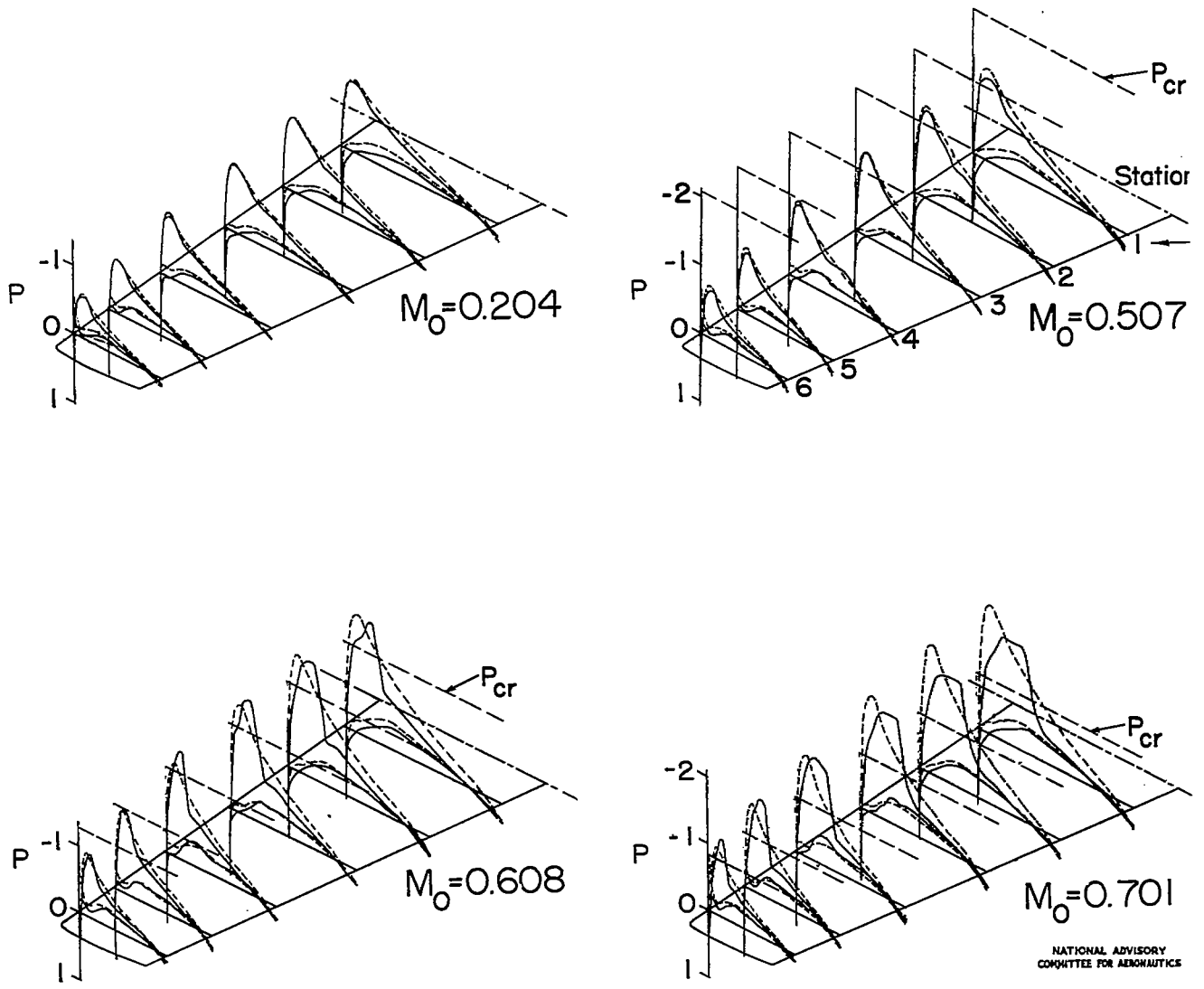

(b) α = 4.5°.

Figure 7.- Continued .

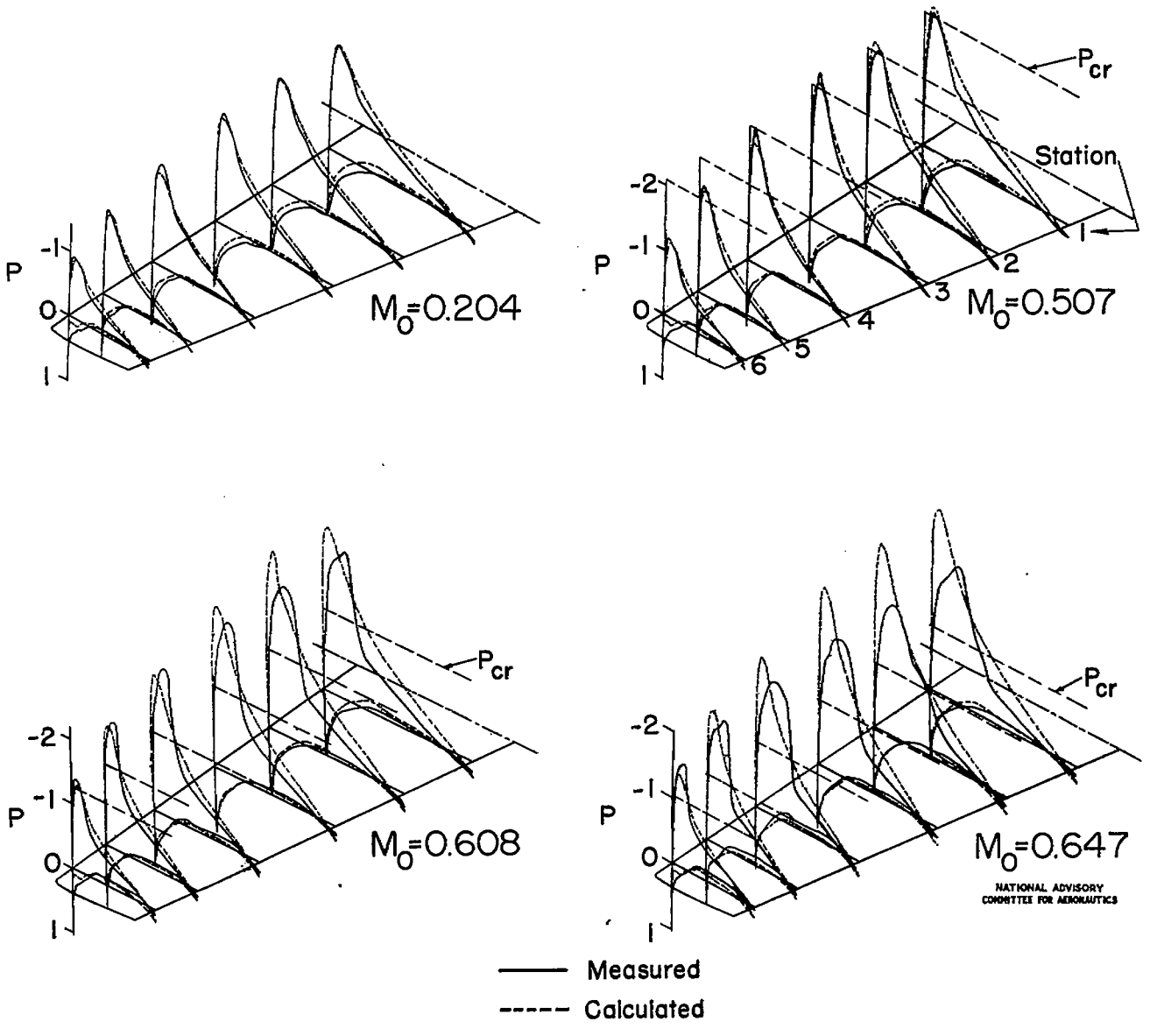

(c) $\alpha = 8.9°$.

Figure 7. - Continued.

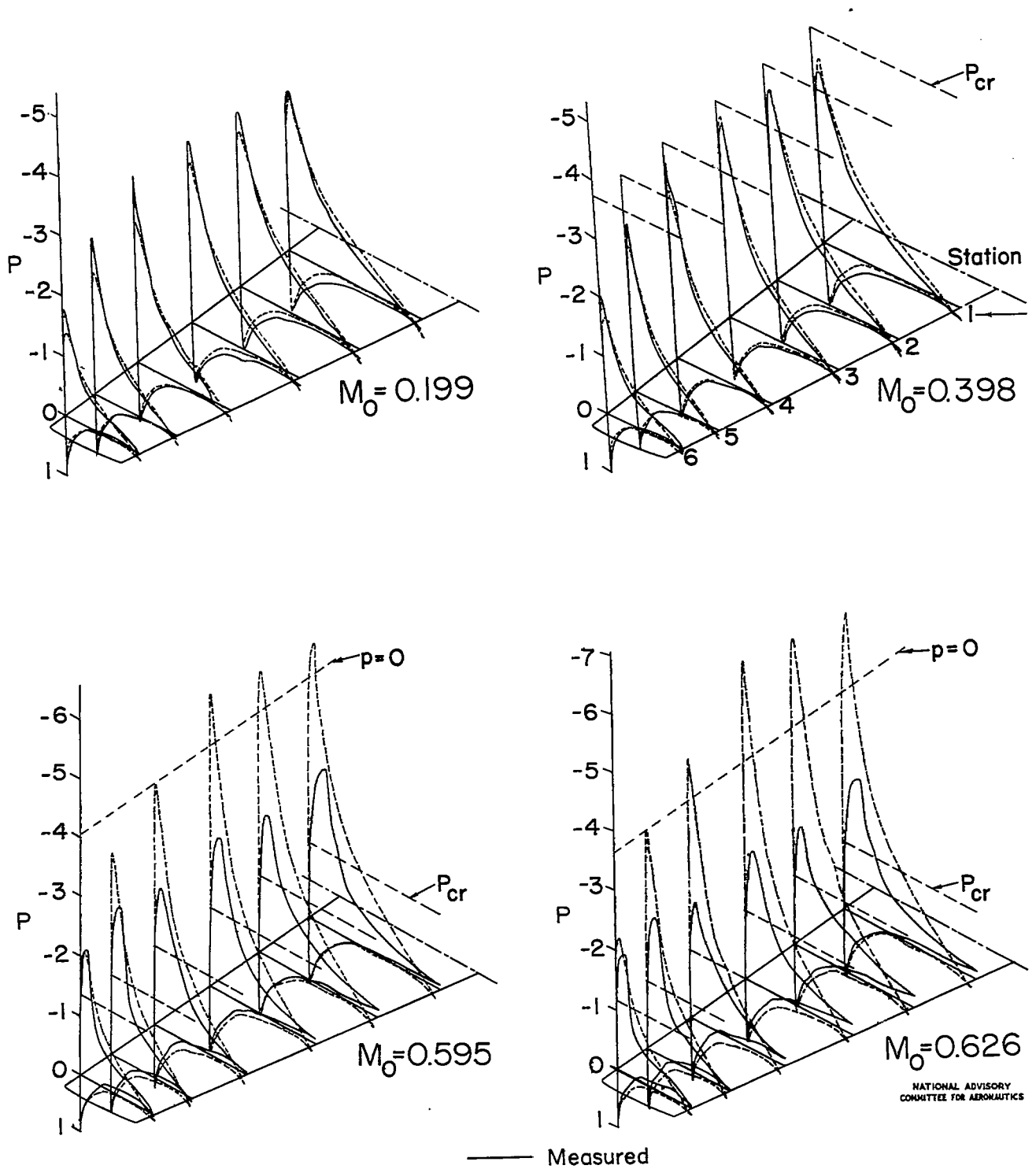

(d) α = 13.2°.

Figure 7.- Continued.

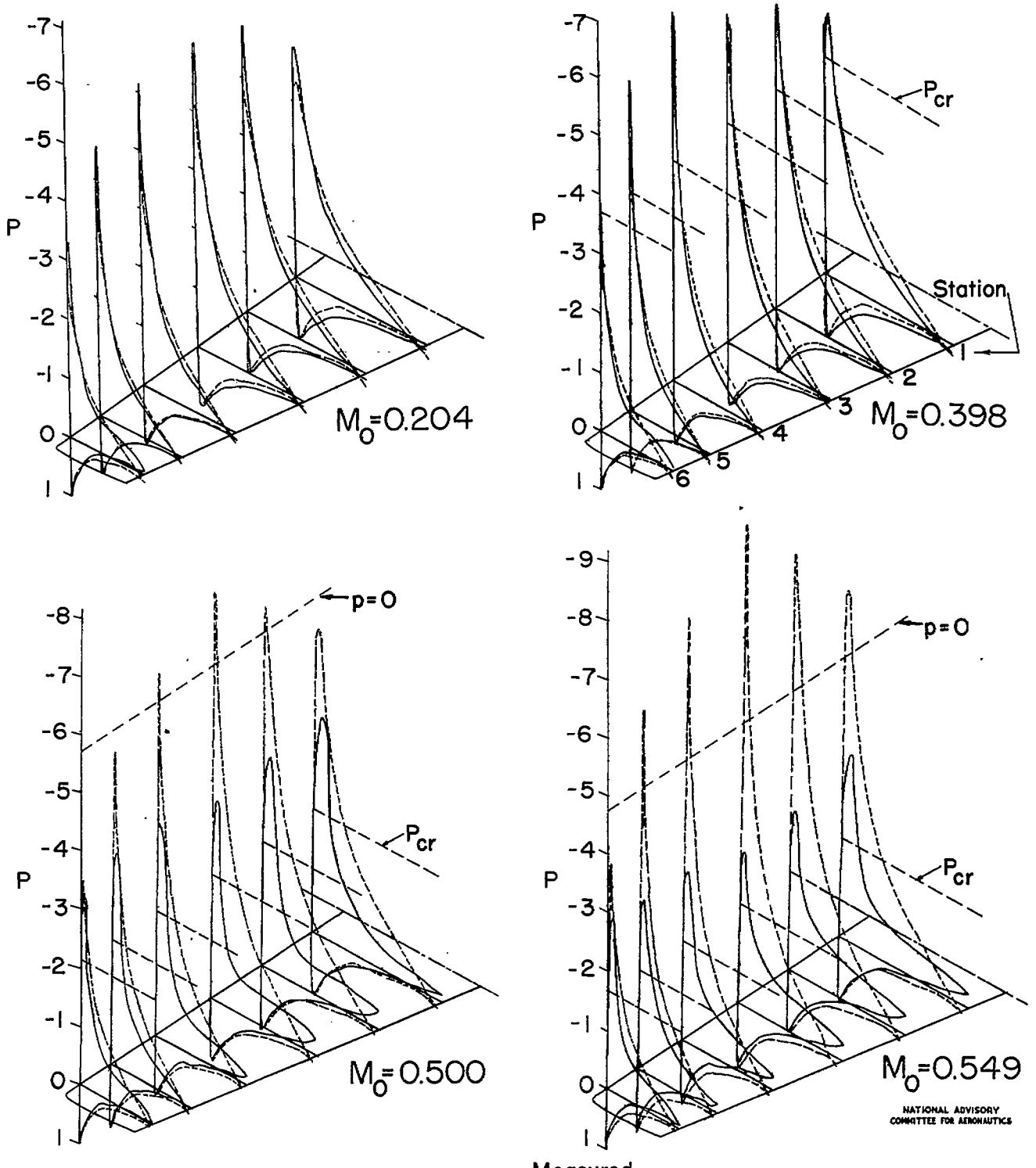

(e) $\alpha = 17.5°$.

Figure 7.- Continued.

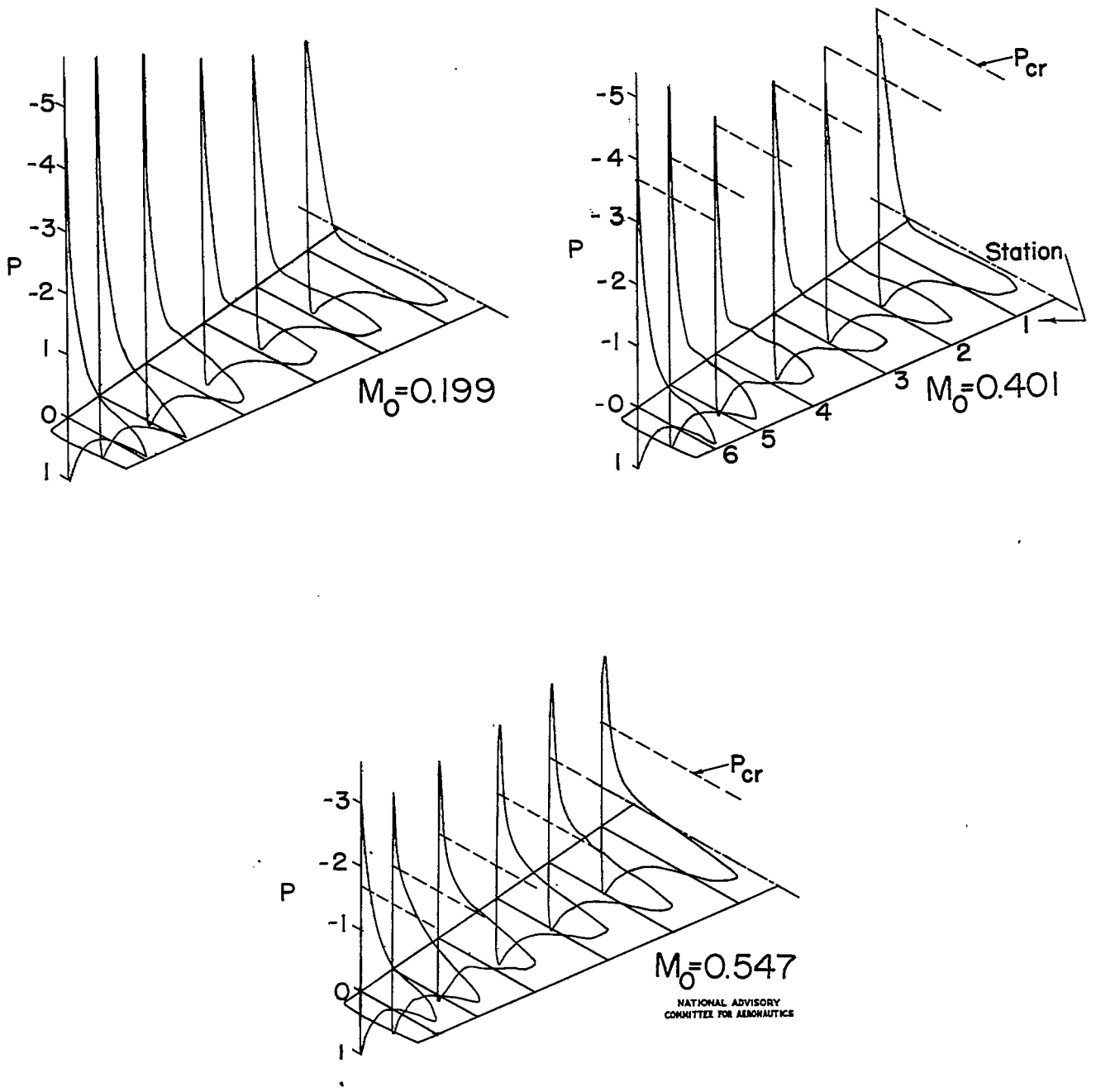

Figure 7.- Concluded.